

# Electrical and interfacial properties of Ag/bulk ZnO Schottky diodes

HOGYOUNG KIM\*

Department of Optometry, Seoul National University of Science and Technology (Seoultech), Seoul 139-743, Korea

The effect of interface states in Ag Schottky contacts on Zn-polar and O-polar bulk ZnO was investigated using current–voltage ( $I$ - $V$ ) measurements. Compared with Zn-polar ZnO, the barrier height was higher and the series resistance was lower for O-polar ZnO. The ideality factor versus voltage plot showed a peak for Zn-polar ZnO, which was associated with an interface state effect. The interface state density, calculated from  $I$ - $V$  characteristics, was higher for Zn-polar ZnO. The results suggested that the hydrogen-related defects in Zn-polar ZnO were attributed to the high density of interface states.

(Received July 2, 2013; accepted November 7, 2013)

**Keywords:** Hydrogen-related defects, Interface states, Series resistance

## 1. Introduction

ZnO is a promising photonics material for various applications, including light emitting diodes (LEDs), laser diodes (LDs), and ultraviolet (UV) photodetectors, due to its wide band gap (3.4 eV at 300 K), high exciton binding energy (60 meV), and excellent radiation hardness [1,2]. Currently, three main techniques are used to grow bulk ZnO single crystals: the hydrothermal, pressurized melt-grown and chemical vapor transport methods [2]. These three methods use different growth mechanisms, resulting in bulk ZnO crystals grown with dissimilar crystalline quality and intrinsic defect density. Various crystalline defects, such as dislocations and vacancies, can also be incorporated into the ZnO layer. These impurities and/or defects will affect the crystalline quality of subsequent epitaxial films on ZnO substrates.

Reliable and reproducible Schottky contacts are needed to realize high-performance ZnO devices. It was shown that the thermal stability of the Ag/n-ZnO Schottky contacts is higher than that of Au/n-ZnO Schottky contacts [3]. Polarity-dependent barrier heights for the Zn-polar (0001) and O-polar (000 $\bar{1}$ ) surfaces were associated with the existence of nonzero net dipole moments perpendicular to the surfaces [4]. The responsivity of Pt Schottky photodiodes was observed to be two times higher on the Zn-polar surface than on the O-polar surface [5]. However, there are few reports concerning the density of interface states in ZnO Schottky diodes [6,7], especially for bulk ZnO. In this work, the effect of interface states on the electrical properties of Ag/bulk ZnO Schottky diodes was investigated using current–voltage measurements.

## 2. Experimental

An unintentionally doped, pressurized melt-grown, Zn-polar and O-polar bulk ZnO single-crystal wafer

(Cermet Inc.) was used in this investigation. The wafer was  $5 \times 5 \times 0.5 \text{ mm}^3$  with a single side polished by the manufacturer. The room-temperature carrier concentration assessed by Hall-effect measurements was  $\sim 1 \times 10^{17} \text{ cm}^{-3}$ . Before metallization, the sample was ultrasonically cleaned for 5 min using acetone and methanol. The sample was rinsed in de-ionized (DI) water and blown dry with  $\text{N}_2$  gas. For the Schottky contact, 50-nm-thick Ag metal was deposited onto the polished side of both samples using radio-frequency (RF) magnetron sputtering (Korea Vacuum Tech., Ltd.); the deposition occurred through a shadow mask with an exposed diameter of 200  $\mu\text{m}$ . RF sputtering was performed at a working pressure of 8 mTorr, an RF power of 50 W, and an Ar gas flow rate of 50 sccm, resulting in an Ag deposition rate of  $\sim 20 \text{ nm min}^{-1}$ . Ohmic contacts were produced by rubbing In metal onto the entire back surface. Current–voltage ( $I$ - $V$ ) measurements were performed on the Schottky contacts for both polar faces with a HP 4156B semiconductor parameter analyzer.

## 3. Results and discussion

Fig. 1 shows the semilogarithmic  $I$ - $V$  characteristics measured at room temperature. The forward bias characteristics of a Schottky diode are given by the following equations using the thermionic emission (TE) model [8]:

$$I = I_0 [\exp(q(V - IR_s) / nk_B T) - 1], \quad (1)$$

$$I_0 = AA^{**} T^2 \exp(-q\phi_b^{eff} / k_B T), \quad (2)$$

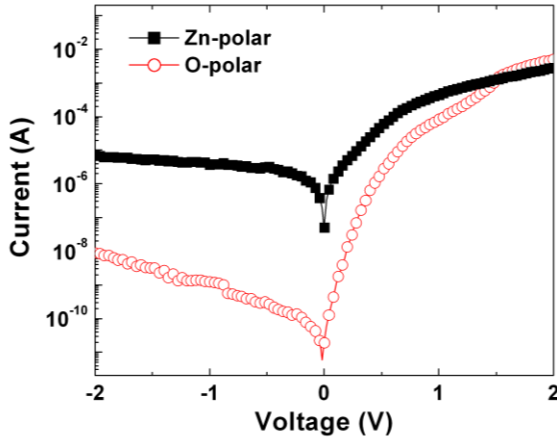


Fig. 1. Current–voltage ( $I$ – $V$ ) characteristics for both samples.

where  $I_0$  is the reverse bias saturation current,  $A$  is the device area,  $A^{**}$  is the effective Richardson constant ( $32 \text{ Acm}^{-2} \text{ K}^{-2}$  for n-ZnO),  $\phi_B^{\text{eff}}$  is the effective Schottky barrier height,  $n$  is the ideality factor,  $V$  is the applied voltage, and  $R_S$  is the series resistance. For values of  $V$  greater than  $3k_B T/q$ , the ideality factor can be obtained from the slope of the linear region of the  $\ln(I)$ – $V$  curves under a forward bias. The forward-biased  $I$ – $V$  analyses for the Zn-polar ZnO revealed that  $\phi_B^{\text{eff}(I-V)} = 0.53 (\pm 0.03) \text{ eV}$ , and  $n = 3.38 (\pm 0.23)$ . Similarly, the analyses for the O-polar ZnO showed that  $\phi_B^{\text{eff}(I-V)} = 0.76 (\pm 0.05) \text{ eV}$ , and  $n = 1.75 (\pm 0.27)$ . The ideality factor at room temperature was much larger than unity, which implies that the current transport cannot be explained by the pure TE model. Such a phenomenon has been attributed to the presence of interfacial states and an insulator layer between the metal and semiconductor [9] and to the prevalence of tunneling and the influence of deep recombination centers [10]. Values of  $n$  greater than unity were also attributed to image force lowering and lateral contact inhomogeneity [11]. Fig. 1 shows the forward-biased  $I$ – $V$  characteristics of the samples; in the high-voltage region, the data deviated from linearity due to factors such as series resistance.

The series resistance is an important parameter in the electrical characteristics of Schottky barrier diodes because it limits the conduction process. According to Cheung's model, the series resistance can be determined from the slope of the following equations [12]:

$$dV/d(\ln I) = nk_B T/q + IR_S, \quad (3)$$

$$H(I) = V - (nk_B T/q) \ln(I/AA^{**}T^2), \quad (4)$$

where  $H(I)$  is given by  $H(I) = n\phi_B + IR_S$ . Fig. 2 shows the  $dV/d(\ln I)$  vs.  $I$  and  $H(I)$  vs.  $I$  plots for both samples. The values of  $R_S$  obtained from the  $dV/d(\ln I)$  vs.  $I$  and  $H(I)$  vs.  $I$  plots were  $355 (\pm 23) \Omega$  ( $143 (\pm 12) \Omega$ ) and  $322 (\pm$

$29) \Omega$  ( $171 (\pm 9.0) \Omega$ ), respectively, for Zn-polar ZnO (O-polar ZnO). The  $R_S$  values for Zn-polar ZnO were higher than those for O-polar ZnO. The presence of an interfacial layer and possibly interface states may contribute to the higher series resistance for Zn-polar ZnO.

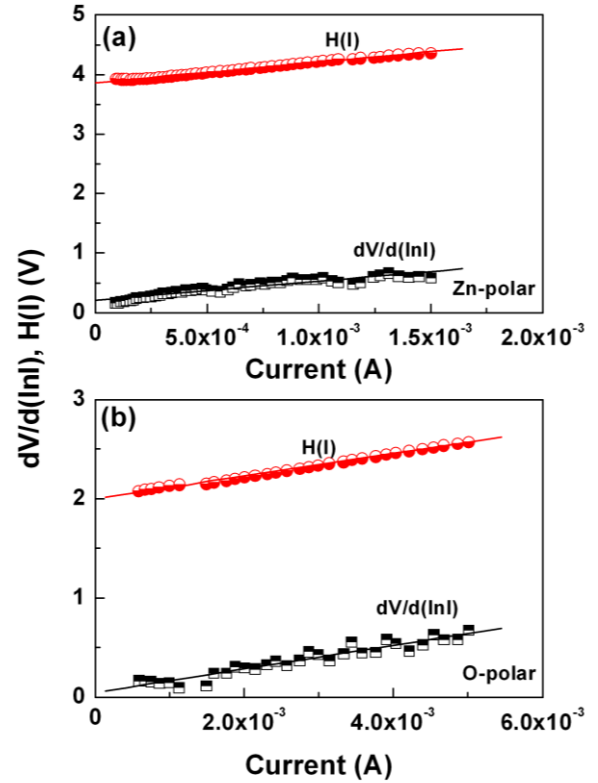


Fig. 2. Plots of  $dV/d(\ln I)$  vs.  $I$  and  $H(I)$  vs.  $I$  for the Ag Schottky contacts to (a) Zn-polar, (b) O-polar ZnO.

In Fig. 3, the forward bias  $\log I$ – $\log V$  curve is characterized by three distinct linear regions, exhibiting the power law behavior of  $I \sim V^m$ , where  $m$  is the slope of each region. For Zn-polar ZnO, the  $m$  values were  $1.12 (\pm 0.4)$ ,  $2.91 (\pm 0.75)$ , and  $2.76 (\pm 0.30)$  for regions I, II, and III, respectively. For O-polar ZnO, the  $m$  values were  $1.27 (\pm 0.15)$ ,  $5.25 (\pm 0.58)$ , and  $3.91 (\pm 0.43)$  for regions I, II, and III, respectively. The  $m$  values obtained for region I corresponded to ohmic behavior (linear dependence). In this region, the injection of carriers from the electrodes into the semiconductor material was reduced considerably due to the low bias voltage [13]. In region II, the current increased exponentially as  $I \sim \exp(cV)$ ; the  $m$  values obtained indicated the presence of trapped charge-limited current (TCLC) mechanisms [14]. In region II, the current was controlled by the exponential distribution of interface states within the band gap of the ZnO layer. In this case, the increase in the number of injected electrons caused the traps to fill, resulting in an increase in the space charge [15]. At high voltages (region III), the slope tended to decrease as the device approached the “trap-filled” limit (i.e., the current reached a trap-free, space-charge limit current (SCLC) for high injection levels that exhibited a

similar dependence on the voltage as that for the TCLC [16]). In this region, the increase in the current was not as significant as the voltage increased. This suggests that most of the traps were filled and that the contribution of free carriers to the electric field became appreciable [17].

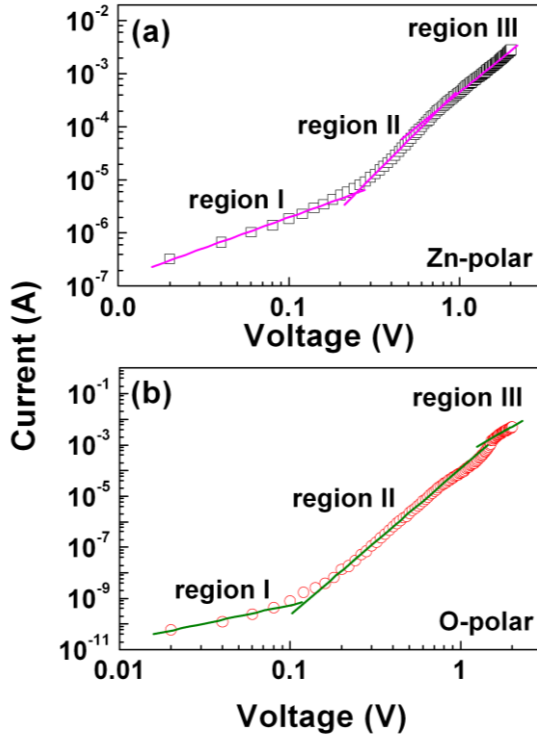


Fig. 3. Log–log plots for the forward-biased  $I$ – $V$  data obtained from (a) Zn-polar and (b) O-polar ZnO.

The bias voltage-dependent ideality factor  $n(V)$  can be obtained from Eq. (1), with an approximation of  $R_S = 0$  [8,18]. The actual form of  $n(V)$  requires the solution of the differential equation

$$\frac{k_B T}{q} \frac{d(\ln I)}{dV} = \frac{1}{n(V)} - \frac{V}{n(V)^2} \frac{dn(V)}{dV}, \quad (5)$$

The conventional linear approximation of  $\ln(I)$ – $V$  neglects the second term on the right side of Eq. (5), which implies the condition  $dn/dV = 0$  [19]. Then,  $n(V)$  can simply be expressed as

$$n(V) = q / k_B T [dV / d(\ln I)], \quad (6)$$

Using Eq. (6), the bias-dependent ideality factors were calculated and are presented in Fig. 4. The data clearly indicate that the diode has ideality factor values larger than unity. For O-polar ZnO,  $n$  increased monotonically with increasing bias voltage, although there was a slight kink at  $\sim 0.5$  V. For Zn-polar ZnO,  $n$  increased with the bias voltage from 1 up to a maximum at  $\sim 0.25$  V and then

decreased. With a further increase in the bias voltage,  $n$  increased again monotonically. The peak in the  $n(V)$  versus voltage plot was observed in other semiconductors, such as GaAs [20] and InP [21], and was attributed to an interface state effect. When the same mechanism is applied to this work, it implies that the interface state density for Zn-polar ZnO was higher than that for O-polar ZnO.

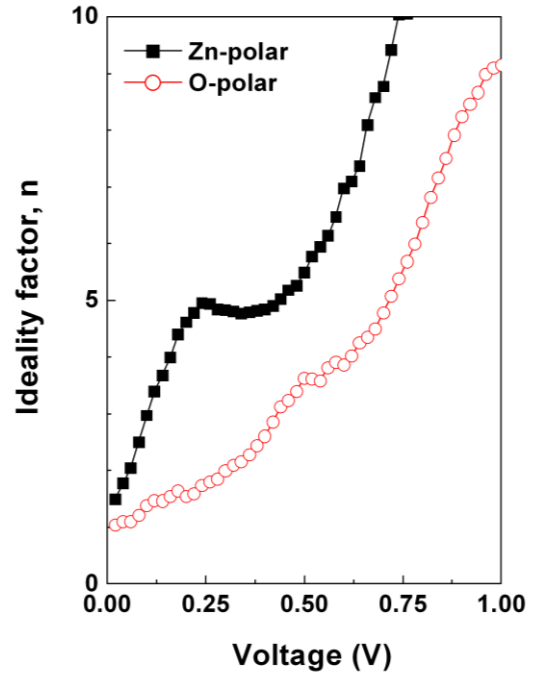


Fig. 4. Bias voltage-dependent ideality factors for both samples.

The density distribution of the interface states ( $N_{SS}$ ) in equilibrium with the semiconductor can be determined from the forward-biased ( $I$ – $V$ ) data by considering the voltage dependent ideality factor  $n(V)$  and the effective barrier height  $\phi_e$ , given by [18]

$$\phi_e = \phi_B^{eff} + \left(1 - \frac{1}{n(V)}\right)(V - IR_S), \quad (7)$$

The ideality factor, which is voltage and temperature dependent, is related to the interfacial layer thickness and density of interface states through the relationship [9]

$$n(V, T) = 1 + \frac{\delta}{\epsilon_0 \epsilon_i} \left[ \frac{\epsilon_0 \epsilon_s}{W_D} + qN_{SS}(V, T) \right], \quad (8)$$

where  $W_D$  is the depletion layer width at zero voltage,  $N_{SS}$  is the density of interface states,  $\epsilon_0$  is the permittivity in vacuum, and  $\epsilon_i$  and  $\epsilon_s$  are the dielectric constants of the interfacial layer of thickness  $\delta$  (assuming about 2 nm) and the semiconductor (8.5 for ZnO [4]), respectively. Due to the Ag–O reaction, the interfacial layer can be expected to

be  $\text{Ag}_2\text{O}$ . In this respect, an  $\varepsilon_i$  value of 11.0 was used for the calculations, which was selected from the literature that reported the dielectric constant of  $\text{Ag}_2\text{O}$  as 11.0 [22]. The measured capacitance is connected to the reverse bias ( $V_r$ ) through the relationship  $A^2/C^2 = 2((V_{bi} - V_r)/qN_d\varepsilon_s\varepsilon_0)$  [8]; here,  $V_{bi}$  is the zero-bias built-in potential, which can be determined from the flat-band voltage for which  $A^2/C^2 = 0$  holds, and  $N_d$  is the donor concentration.  $V_{bi}$  and  $N_d$  were first obtained from the capacitance–voltage ( $C$ – $V$ ) characteristics measured at 100 kHz. Then, the depletion layer widths at zero bias ( $W_D$ ) were calculated using  $W_D = \sqrt{2\varepsilon_0\varepsilon_s V_{bi}/qN_D}$ . The  $W_D$  values for the measured Schottky diodes were estimated to be ~60–70 nm and ~80–90 nm, respectively, for Zn-polar and O-polar ZnO. For an  $n$ -type semiconductor, the energy difference between the conduction band minimum,  $E_C$ , and the energy of the interface states,  $E_{SS}$ , at the surface of the semiconductor is given by the following [23]:

$$E_C - E_{SS} = (\phi_e - q(V - IR_s)), \quad (9)$$

The density of interface states is extracted using the ideality factor values, as determined from the linear region of forward  $\ln(I)$  vs.  $(V - IR_s)$  characteristics, where the forward applied voltage is greater than  $3k_B T/q$ . Fig. 5 shows the energy-distribution profile of  $N_{SS}$  at room temperature; the  $N_{SS}$  value decreased with increasing  $E_C - E_{SS}$  value. The change in the charge of the interface states, and thus the energy distribution of the interface states due to the potential drop across the interfacial layer, varied with the bias voltage. This alters the diffusion potential and therefore the depletion capacitance [8,18]. Aydođan *et al.* and Yakuphanoglu obtained values of  $17.3 \times 10^{13} \text{ eV}^{-1}\text{cm}^{-2}$  and  $1.2\text{--}1.8 \times 10^{12} \text{ eV}^{-1}\text{cm}^{-2}$ , respectively, for Au/ $n$ -ZnO Schottky contacts on  $n$ -Si [6,7]. Recently, Hussain *et al.* reported a value of  $2 \times 10^{13} \text{ eV}^{-1}\text{cm}^{-2}$  for Au/ZnO nanorod Schottky diodes [13]. In this work, the density of interface states varied from  $7.80 \times 10^{13} \text{ eV}^{-1}\text{cm}^{-2}$  at  $(E_C - 0.36) \text{ eV}$  to  $6.40 \times 10^{13} \text{ eV}^{-1}\text{cm}^{-2}$  at  $(E_C - 0.50) \text{ eV}$  for Zn-polar ZnO. For O-polar ZnO, the density of interface states varied from  $5.00 \times 10^{13} \text{ eV}^{-1}\text{cm}^{-2}$  at  $(E_C - 0.36) \text{ eV}$  to  $1.20 \times 10^{13} \text{ eV}^{-1}\text{cm}^{-2}$  at  $(E_C - 0.69) \text{ eV}$ . For simplicity, the average interface state densities at  $E_C - E_{SS} = 0.45 \text{ eV}$  for measured Schottky diodes were calculated. The interface state densities obtained were  $6.29 (\pm 0.72) \times 10^{13} \text{ eV}^{-1}\text{cm}^{-2}$  and  $3.60 (\pm 1.08) \times 10^{13} \text{ eV}^{-1}\text{cm}^{-2}$ , respectively, for Zn-polar and O-polar ZnO. The results indicated that the Zn-polar sample had a higher density of interface states compared with O-polar, which is consistent with the results from the bias-dependent ideality factor, as shown in Fig. 4.

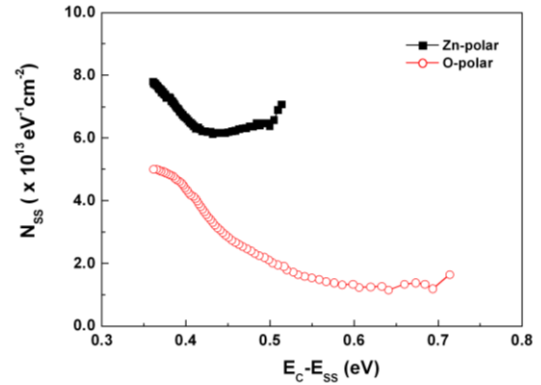


Fig. 5. Energy distribution profiles of interface states obtained from the forward bias  $I$ – $V$  characteristics for both samples.

Based on X-ray photoemission spectroscopy (XPS) measurements, Allen *et al.* showed that hydroxyl (OH) termination is favored for Zn-polar ZnO, whereas H termination is favored for O-polar ZnO [24]. Dong and Brillson suggested that noble metal–oxygen bonds (e.g., Ag–O) can form Schottky contacts, while metal–Zn bonds are associated with ohmic-like contacts [25]. For Zn-polar ZnO, if the Ag atoms are deposited on top of the highly conductive OH layer, then electrons can tunnel directly through the Ag contact, which becomes ohmic in nature. If the kinetic energy of incident Ag atoms from sputtering is sufficient to remove the OH layer, then the formation of Ag–Zn bonds will occur, producing ohmic-like behavior. If the incident Ag atoms break the O–H bonds and only remove H atoms, then Ag–O formation can occur, leading to Schottky-like behavior. Zn-polar ZnO exhibited rectifying  $I$ – $V$  characteristics to some extent (Fig. 1), meaning that the H layer was partially removed. During Ag deposition onto O-polar ZnO, H, rather than OH, could be removed more effectively (breaking a single O–H bond or three O–Zn bonds for H and OH removal, respectively), and subsequent Ag–O formation occurred easily, producing a higher barrier height for O-polar ZnO. Using KrF excimer laser irradiation, the improved rectifying characteristics in Pt/ $n$ -ZnO Schottky diodes was observed and was attributed to the removal of surface carbon and hydrogen contaminants [26]. This means that hydrogen-related defects can act as interface states. Because H atoms were only partially removed for Zn-polar ZnO, the remaining hydrogen contaminants may contribute to the density of interface states more significantly for Zn-polar ZnO. Further investigation is underway to clarify the exact origin of the interface states.

#### 4. Conclusion

Using current–voltage ( $I$ – $V$ ) measurements, the effect of interface states on the electrical properties in Ag/ZnO Schottky contacts were investigated. The barrier height (series resistance) obtained from O-polar ZnO was higher (lower) than that from Zn-polar ZnO. A peak was

observed in the ideality factor versus voltage plot for Zn-polar ZnO associated with an interface state effect. The density of interface states calculated from  $I$ - $V$  characteristics was higher for Zn-polar ZnO, whereas only the H atoms were removed easily for O-polar ZnO. A higher degree of the interfacial Ag-O reaction occurred, which eventually enhanced the barrier height. Consequently, the hydrogen contaminants may be associated with the higher density of interface states for Zn-polar ZnO.

## References

- [1] Ya. Alivov, E. Kalinina, A. Cherenkov, D. Look, B. Ataev, A. Omaev, M. Chukichev, D. Bagnall, *Appl. Phys. Lett.* **83**, 4719 (2013).
- [2] V. Avrutin, G. Cantwell, J. Zhang, J. Song, D. Silversmith, H. Morkoç, *Proceedings of the IEEE* **98**, 1339 (2010).
- [3] J. Simpson, F. Cordaro, *J. Appl. Phys.* **63**, 1781 (1988).
- [4] M. Allen, M. Alkaisi, S. Durbin, *Appl. Phys. Lett.* **89**, 103520 (2006).
- [5] H. Endo, M. Sugibuchi, K. Takahashi, S. Goto, S. Sugimura, K. Hane, Y. Kashiwaba, *Appl. Phys. Lett.* **90**, 121906 (2007).
- [6] Ş. Aydoğan, K. Çınar, H. Asıl, C. Coşkun, A. Türüt, *J. Alloys. Compd.* **476**, 913 (2009).
- [7] F. Yakuphanoglu, *J. Alloys Compd.* **507**, 184 (2010).
- [8] S. Sze, *Physics of Semiconductor Devices*, Wiley, New York (1981).
- [9] H. Card, E. Rhoderick, *J. Phys. D: Appl. Phys.* **4**, 1589 (1971).
- [10] K. Ip, G. Thaler, H. Yang, S. Han, Y. Li, D. Norton, S. Pearton, S. Jang, F. Ren, *J. Cryst. Growth* **287**, 149 (2006).
- [11] R. Tung, *Mater. Sci. Eng. R* **35**, 1 (2001).
- [12] S. Cheung, N. Cheung, *Appl. Phys. Lett.* **49**, 85 (1986).
- [13] I. Hussain, M. Soomro, N. Bano, O. Nur, M. Willander, *J. Appl. Phys.* **113**, 234509 (2013).
- [14] H. Uslu, S. Altındal, I. Polat, H. Bayrak, E. Bacaksız, *J. Alloys. Compd.* **509**, 5555 (2010).
- [15] S. Ocak, M. Kulakcı, T. Kılıcıoğlu, R. Turan, K. Akkılıc, *Synth. Met.* **159**, 1603 (2009).
- [16] T. Kılıcıoğlu, M. Aydın, G. Topal, M. Ebeoğlu, H. Saygılı, *Synth. Met.* **157**, 540 (2007).
- [17] D. Lile, in: *Physics and Chemistry of III-V Compound Semiconductor Interfaces*, Ed. C. Wilmsen, Plenum Press, New York (1985).
- [18] E. Rhoderick, R. Williams, *Metal Semiconductor Contacts*, Clarendon, Oxford (1981).
- [19] V. Mikhelashvili, G. Eisenstein, R. Uzdin, *Solid-State Electron.* **45**, 143 (2001).
- [20] K. Maeda, H. Ikoma, T. Ischida, *Appl. Phys. Lett.* **62**, 2560 (1993).
- [21] A. Ahaitouf, A. Bath, E. Losson, E. Abarkan, *Mater. Sci. Eng. B* **52**, 208 (1998).
- [22] K. Chatterjee, S. Banerjee, D. Chakravorty, *Phys. Rev. B* **66**, 085421 (2002).
- [23] S. Demirezen, Z. Sönmez, U. Aydemir, Ş. Altındal, *Curr. Appl. Phys.* **12**, 266 (2012).
- [24] M. Allen, D. Zemlyanov, G. Waterhouse, J. Metson, T. Veal, C. McConville, S. Durbin, *Appl. Phys. Lett.* **98**, 101906 (2011).
- [25] Y. Dong, L. Brillson, *J. Electron. Mater.* **37**, 743 (2007).
- [26] M. Oh, D. Hwang, J. Lim, Y. Choi, S. Park, *Appl. Phys. Lett.* **91**, 042109 (2007).

\* Corresponding author: hoyoungkim@gmail.com